Appl. Phys. B 74, 697–703 (2002)
DOI: 10.1007/s003400200837

Applied Physics B
Lasers and Optics

R. ATKINSON✉
N.F. KUBRAKOV*

Features of the simplest model of second-harmonic magneto-optical Kerr effects

Department of Pure and Applied Physics, The Queen's University of Belfast, Belfast BT7 1NN, Northern Ireland, UK

Received: 16 October 2001
Published online: 24 April 2002 •

ABSTRACT A generalised formalism of characteristic matrices is presented to analyse second-harmonic magneto-optical Kerr effects in an optically anisotropic centrosymmetric ferromagnetically ordered multilayer if its response can be described in terms of electric polarisation. Features of the model associated with ideal (infinitely thin) interfaces are highlighted. These are due to both the existence of two versions of unconventional boundary conditions and an inevitable conventional approach to defining the surface polarisations through the fundamental electric field and surface-susceptibility tensors. New analytical results for linear and second-harmonic Kerr effects are shown to be advantageous for developing an effective algorithm for their numerical simulation. The linear approximation with respect to magnetisation is pursued, thereby also making our results suitable for investigating a great variety of magneto-optical effects and (in the second-harmonic case) effects related to anisotropy.

PACS 78.20.Ls; 78.20.Bh; 78.20.Ci; 42.65.-k; 03.50.De

1 Introduction

The interaction of intense laser radiation of frequency ω with a magnetic multilayer may result in magneto-optical (MO) effects at the frequencies ω and $\omega_S = 2\omega$ [1–3]. When observed in reflected light these effects are respectively referred to as linear and second-harmonic MO Kerr effects (MOKE and SHMOKE). The phenomenological model [1–5] commonly used to describe them is based on a number of assumptions that do not necessarily lead to an inadequate interpretation but greatly simplify the analysis. We shall show its features and provide new analytical results for the case of an optically isotropic centrosymmetric magnetic multilayer – a set of layers composed of different materials on a nonmagnetic substrate (Fig. 1). Interfaces, including that between the first layer and the nondispersive transparent medium of frequency-independent refractive index n_0, are assumed so narrow (their width is much smaller than the wavelength) that they may be thought of as ideal surfaces infinitely extended in the film plane. The laser radiation incident on the multilayer at the angle φ is regarded as a plane wave whose state of polarisation is known. The response of the multilayer is governed entirely by electric (effective) polarisations distributed in the volume regions and at the surfaces. Four kinds of polarisations result. Linear volume polarisation $\boldsymbol{P}^{\mathrm{LV}}$ accounts for conventional MOKE, and linear surface $\boldsymbol{P}^{\mathrm{LS}}$ for its surface counterpart, i.e. surface MOKE (SMOKE) [5, 6], induced exclusively at the interfaces. Nonlinear volume polarisation $\boldsymbol{P}^{\mathrm{NV}}$ and surface $\boldsymbol{P}^{\mathrm{NS}}$ give rise to volume- and surface-sensitive SHMOKE. Compared with $\boldsymbol{P}^{\mathrm{LV}}$, the other three kinds of polarisations are small enough to be treated as perturbations. They all are related to the fundamental electric field in the layers through susceptibility tensors. To determine the reflected and second-harmonic waves in the transparent medium and then the MO effects themselves, the formalism of characteristic matrices, based on the Maxwell equations and certain boundary conditions, can be used advantageously [5].

Such a simple model features two subtleties that are likely to cause ambiguity. First, there exist two versions of the boundary conditions involving surface polarisation, and this is due to two possible options of defining the electric induction at an interface [7]. Second, the way one defines $\boldsymbol{P}^{\mathrm{LS}}$ and $\boldsymbol{P}^{\mathrm{NS}}$ in terms of the fundamental field at the interface is a matter of convention as a result of discontinuity of the normal component of this field. Several distinct conventions may be encountered and they are all valid. However, they may lead to different values of the surface-susceptibility tensors. Since these aspects of the model need careful handling, we devote this paper to a detailed analysis of MOKE and SHMOKE. Consideration of SMOKE is very similar [5]. A particular set of boundary conditions and a clearly defined convention will be pursued. SI units will be used throughout. In Sect. 2, we will briefly outline the formalism of dealing with the reflected wave at the fundamental frequency and consequently MOKE. Important expressions for the longitudinal, polar, and transverse configurations will be given. Extension of this formalism to the problem of treating the second-harmonic wave and SHMOKE will be described in Sect. 3. This will be based on our preferred conventional definition for the nonlinear surface polarisation in terms of corresponding susceptibility tensor

✉ E-mail: ronald.atkinson@qub.ac.uk
**Permanent address:* Theoretical Department, General Physics Institute of Russian Academy of Science, 38 Vavilov St., Moscow 117942, Russia

and fundamental field. Decomposition of the tensor in the linear approximation with respect to magnetisation [7] will allow us to obtain analytical results especially suitable for looking at rotational anisotropy of SHMOKE. We shall show how the characteristic matrix formalism is modified by the unconventional boundary conditions, leading to analytical results for the second-harmonic wave in the transparent medium. Section 4, apart from a summary of our analysis, addresses the relationship between possible conventions (rescaling procedure for tensor components) and alternative boundary conditions to make our result consistent with those that come from both different conventions and a different set of the boundary conditions.

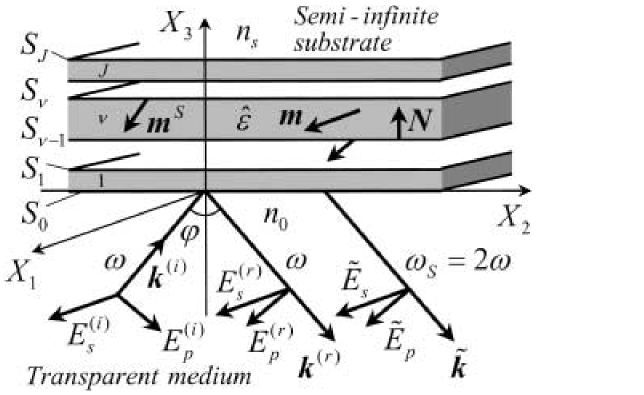

FIGURE 1 Multilayer configuration for the model of MO effects.

2 Reflected wave and MOKE

Here initial results of our analysis of MOKE in the multilayer (Fig. 1) by means of the characteristic matrix formalism are outlined so that a similar analysis of SHMOKE (in Sect. 3) might be followed more easily.

The electric field $\boldsymbol{E}^{(i)}$ and the magnetic field $\boldsymbol{H}^{(i)}$ of the incident wave can be expressed in terms of the s- and p-components of $\boldsymbol{E}^{(i)}$ defined at the surface of the multilayer:

$$\boldsymbol{E}^{(i)} = \exp\left(\mathrm{i}\left(\boldsymbol{k}^{(i)}, \boldsymbol{x}\right)\right)\left(E_s^{(i)},\ n_0^{-1}\zeta E_p^{(i)}, -n_0^{-1}\alpha E_p^{(i)}\right),$$
$$\boldsymbol{H}^{(i)} = -Z^{-1}\exp\left(\mathrm{i}\left(\boldsymbol{k}^{(i)}, \boldsymbol{x}\right)\right)\left(n_0 E_p^{(i)},\ -\zeta E_s^{(i)}, \alpha E_s^{(i)}\right),$$

where $\boldsymbol{k}^{(i)} = k_0(0, \alpha, \zeta)$ is the wave vector, $k_0 = \omega/c$ the wave number, c the velocity of light in vacuum, $\alpha = n_0 \sin\varphi$, $\zeta = n_0 \cos\varphi$, n_0 the refractive index of the transparent medium, φ the angle of incidence, and $Z = (\mu_0 \varepsilon_0^{-1})^{1/2}$ the wave impedance of vacuum. Owing to the conventional boundary conditions, any wave propagating in the layer inherits the structure and properties of the incident wave. All the wave vectors have the same first and second components, which coincide with those of $\boldsymbol{k}^{(i)}$.

Within the linear approximation in magnetisation [7], an optically isotropic layer homogeneously magnetised along the unit vector $\boldsymbol{m}$ is introduced into the wave equation by the permittivity tensor

$$\varepsilon_{ij}(\omega) = n^2\left(\delta_{ij} - \mathrm{i}Q e_{ijk} m_k\right), \tag{1}$$

where n is the complex refractive index ($\mathrm{Im}\, n > 0$ because of the implicated time-dependent factor $\exp(-\mathrm{i}\omega t)$), Q the complex magneto-optical parameter, and δ_{ij} and e_{ijk} are the Kronecker delta and the permutation symbol (Levi–Civita tensor), respectively. More commonly the tensor (1) is given in matrix form:

$$\hat{\varepsilon}(\omega) = n^2\begin{bmatrix} 1 & -\mathrm{i}Qm_3 & \mathrm{i}Qm_2 \\ \mathrm{i}Qm_3 & 1 & -\mathrm{i}Qm_1 \\ -\mathrm{i}Qm_2 & \mathrm{i}Qm_1 & 1 \end{bmatrix}.$$

Let $\boldsymbol{N} = (0, 0, 1)$ be a unit normal to each interface (Fig. 1). We shall use the superscript '+' to refer to that side of an interface, which is defined as positive by a positive direction of $\boldsymbol{N}$. Quantities defined at the other side are labelled with '−'. By definition, the characteristic matrix $\hat{\boldsymbol{M}}$ of a layer relates the vector $\left(\mathcal{E}_1^-, Z\mathcal{H}_2^-, \mathcal{E}_2^-, Z\mathcal{H}_1^-\right)^{\mathrm{T}}$ at the interface, which is set further from the transparent medium, to the similar vector $\left(\mathcal{E}_1^+, Z\mathcal{H}_2^+, \mathcal{E}_2^+, Z\mathcal{H}_1^+\right)^{\mathrm{T}}$ at the other interface, i.e. $\left(\mathcal{E}_1^+, Z\mathcal{H}_2^+, \mathcal{E}_2^+, Z\mathcal{H}_1^+\right)^{\mathrm{T}} = \hat{\boldsymbol{M}}\left(\mathcal{E}_1^-, Z\mathcal{H}_2^-, \mathcal{E}_2^-, Z\mathcal{H}_1^-\right)^{\mathrm{T}}$ Here the tangential components of electric and magnetic fields are defined internally with respect to the layer. By virtue of the conventional boundary conditions, it is also appropriate to define these components externally. The characteristic matrix has the following distinctive symmetry:

$$\hat{\boldsymbol{M}} = \hat{\boldsymbol{M}}^{(0)} + Q\hat{\boldsymbol{M}}^{(1)} = \begin{bmatrix} m_{11} & m_{12} & 0 & 0 \\ m_{21} & m_{11} & 0 & 0 \\ 0 & 0 & m_{11} & m_{34} \\ 0 & 0 & m_{43} & m_{11} \end{bmatrix} + Q\begin{bmatrix} 0 & 0 & \tilde{m}_{13} & \tilde{m}_{14} \\ 0 & 0 & \tilde{m}_{23} & \tilde{m}_{24} \\ \tilde{m}_{24} & \tilde{m}_{14} & \tilde{m}_{33} & 0 \\ \tilde{m}_{23} & \tilde{m}_{13} & 0 & -\tilde{m}_{33} \end{bmatrix} \tag{2}$$

and 10 independent components [5]

$$\begin{aligned}
&m_{11} = \cosh\mu,\ m_{12} = -\gamma^{-1}\sinh\mu,\ m_{21} = -\gamma\sinh\mu,\\
&m_{34} = n^{-2}\gamma\sinh\mu,\ m_{43} = n^2\gamma^{-1}\sinh\mu,\\
&\tilde{m}_{33} = \mathrm{i}m_1\alpha\gamma^{-1}\sinh\mu,\\
&\tilde{m}_{13} = 1/2\,\mathrm{i}m_2\alpha n^2\gamma^{-3}(\mu\cosh\mu - \sinh\mu)\\
&\quad - 1/2\,\mathrm{i}m_3 n^2\gamma^{-2}\mu\sinh\mu,\\
&\tilde{m}_{14} = 1/2\,\mathrm{i}m_2\alpha\gamma^{-2}\mu\sinh\mu + 1/2\,\mathrm{i}m_3\gamma^{-1}(\sinh\mu - \mu\cosh\mu),\\
&\tilde{m}_{23} = -1/2\,\mathrm{i}m_2\alpha n^2\gamma^{-2}\mu\sinh\mu\\
&\quad + 1/2\,\mathrm{i}m_3 n^2\gamma^{-1}(\sinh\mu + \mu\cosh\mu),\\
&\tilde{m}_{24} = -1/2\,\mathrm{i}m_2\alpha\gamma^{-1}(\mu\cosh\mu + \sinh\mu) + 1/2\,\mathrm{i}m_3\mu\sinh\mu,
\end{aligned}$$

where $\mu = \mathrm{i}k_0\gamma h$, $\gamma = (n^2 - \alpha^2)^{1/2}$, h is thickness of the layer, and the other parameters are defined in (1). If the layer is nonmagnetic, $\hat{\boldsymbol{M}}^{(1)}$ disappears. In the characteristic matrix $\hat{\boldsymbol{S}}_\nu = \hat{\boldsymbol{S}}_\nu^{(0)} + \hat{\boldsymbol{S}}_\nu^{(1)}$ of the first ν layers (sets of their parameters may be different) we distinguish its nonmagnetic part $\hat{\boldsymbol{S}}_\nu^{(0)} = \hat{\boldsymbol{M}}_1^{(0)} \cdots \hat{\boldsymbol{M}}_\nu^{(0)}$ and its magnetic part $\hat{\boldsymbol{S}}_\nu^{(1)} = Q_1\hat{\mathbf{M}}_1^{(1)}\hat{\boldsymbol{M}}_2^{(0)} \cdots \hat{\boldsymbol{M}}_\nu^{(0)} + \ldots + Q_j\hat{\mathbf{M}}_1^{(0)} \cdots \hat{\boldsymbol{M}}_{j-1}^{(0)}\hat{\boldsymbol{M}}_j^{(1)}\hat{\boldsymbol{M}}_{j+1}^{(0)} \cdots \hat{\boldsymbol{M}}_\nu^{(0)} + \ldots + Q_\nu\hat{\boldsymbol{M}}_1^{(0)} \cdots \hat{\boldsymbol{M}}_{\nu-1}^{(0)}\hat{\boldsymbol{M}}_\nu^{(1)}$. For the whole multilayer $\hat{\boldsymbol{S}}_J = \hat{\boldsymbol{P}}$, whilst $\hat{\boldsymbol{S}}_0^{(0)}$ and

$\hat{\boldsymbol{S}}_0^{(1)}$ are a unit and a zero matrix respectively. We assume that the substrate is semi-infinite and optically isotropic to be characterised by a single parameter – the complex refractive index n_s. Applying the conventional boundary conditions, the normal modes in the transparent medium and the substrate lead to the following equation:

$$\hat{\boldsymbol{F}}\begin{bmatrix} E_s^{(i)} \\ E_p^{(i)} \\ E_s^{(r)} \\ E_p^{(r)} \end{bmatrix} = \hat{\boldsymbol{P}}\begin{bmatrix} 1 & 0 \\ \gamma_s & 0 \\ 0 & 1 \\ 0 & -n_s^2\gamma_s^{-1} \end{bmatrix}\begin{bmatrix} \mathcal{E}_{01}^+ \\ \mathcal{E}_{02}^+ \end{bmatrix}, \tag{3}$$

where $\hat{\boldsymbol{F}} = \begin{bmatrix} 1 & 0 & 1 & 0 \\ \zeta & 0 & -\zeta & 0 \\ 0 & n_0^{-1}\zeta & 0 & -n_0^{-1}\zeta \\ 0 & -n_0 & 0 & -n_0 \end{bmatrix}$, $\gamma_s = (n_s^2 - \alpha^2)^{1/2}$, and the complex amplitudes on the right-hand side are defined at the last interface. The s- and p-components of the reflected wave become available from (3) and are related to $E_s^{(i)}$ and $E_p^{(i)}$ through the reflection matrix:

$$\begin{bmatrix} E_s^{(r)} \\ E_p^{(r)} \end{bmatrix} = \begin{bmatrix} r_{ss} & r_{sp} \\ r_{ps} & r_{pp} \end{bmatrix}\begin{bmatrix} E_s^{(i)} \\ E_p^{(i)} \end{bmatrix}, \tag{4}$$

which comprises the generalised Fresnel coefficients expressed in terms of $\hat{\boldsymbol{P}}$:

$$r_{ss} = \frac{(p_{11}+p_{12}\gamma_s)\zeta - p_{21} - p_{22}\gamma_s}{(p_{11}+p_{12}\gamma_s)\zeta + p_{21} + p_{22}\gamma_s},$$

$$r_{sp} = \frac{2n_0\zeta\left[\left(\tilde{p}_{13}\gamma_s - \tilde{p}_{14}n_s^2\right)\left(p_{21}+p_{22}\gamma_s\right) - \left(\tilde{p}_{23}\gamma_s - \tilde{p}_{24}n_s^2\right)\left(p_{11}+p_{12}\gamma_s\right)\right]}{\left(\left(p_{11}+p_{12}\gamma_s\right)\zeta + p_{21}+p_{22}\gamma_s\right)\left(\left(p_{33}\gamma_s - p_{34}n_s^2\right)n_0^2 - \left(p_{43}\gamma_s - p_{44}n_s^2\right)\zeta\right)},$$

$$r_{ps} = \frac{2n_0\zeta\left[\left(\tilde{p}_{31}+\tilde{p}_{32}\gamma_s\right)\left(p_{43}\gamma_s - p_{44}n_s^2\right) - \left(\tilde{p}_{41}+\tilde{p}_{42}\gamma_s\right)\left(p_{33}\gamma_s - p_{34}n_s^2\right)\right]}{\left(\left(p_{11}+p_{12}\gamma_s\right)\zeta + p_{21}+p_{22}\gamma_s\right)\left(\left(p_{33}\gamma_s - p_{34}n_s^2\right)n_0^2 - \left(p_{43}\gamma_s - p_{44}n_s^2\right)\zeta\right)},$$

$$r_{pp} = r_{pp}^{(0)} + r_{pp}^{(1)} = \frac{-\left(p_{33}\gamma_s - p_{34}n_s^2\right)n_0^2 - \left(p_{43}\gamma_s - p_{44}n_s^2\right)\zeta}{\left(p_{33}\gamma_s - p_{34}n_s^2\right)n_0^2 - \left(p_{43}\gamma_s - p_{44}n_s^2\right)\zeta} + 2n_0^2\zeta\frac{\left(\tilde{p}_{33}\gamma_s - \tilde{p}_{34}n_s^2\right)\left(p_{43}\gamma_s - p_{44}n_s^2\right) - \left(\tilde{p}_{43}\gamma_s - \tilde{p}_{44}n_s^2\right)\left(p_{33}\gamma_s - p_{34}n_s^2\right)}{\left(\left(p_{33}\gamma_s - p_{34}n_s^2\right)n_0^2 - \left(p_{43}\gamma_s - p_{44}n_s^2\right)\zeta\right)^2}.$$

To make sure that these expressions are correct, the symmetry principle for reflection matrices, due to Shelankov and Pikus [8], can be used. In our case, and with regard to the sign convention we use for $\boldsymbol{E}^{(r)}$, this guiding principle states the following:

$$r_{ss}(\varphi; \boldsymbol{m}_1, ..., \boldsymbol{m}_J) = r_{ss}(-\varphi; -\boldsymbol{m}_1, ..., -\boldsymbol{m}_J),$$
$$r_{sp}(\varphi; \boldsymbol{m}_1, ..., \boldsymbol{m}_J) = -r_{ps}(-\varphi; -\boldsymbol{m}_1, ..., -\boldsymbol{m}_J),$$
$$r_{pp}(\varphi; \boldsymbol{m}_1, ..., \boldsymbol{m}_J) = r_{pp}(-\varphi; -\boldsymbol{m}_1, ..., -\boldsymbol{m}_J).$$

For $J = 1$, it can immediately be inferred from (2) that these properties are satisfied.

In the zero approximation with respect to magnetisation (all the Q-parameters are zero), the electric field inside the νth layer can be expressed through the matrix $\hat{\boldsymbol{W}} = \hat{\boldsymbol{M}}_\nu \cdots \hat{\boldsymbol{M}}_J$:

$$\mathcal{E}_1 = 2\zeta E_s^{(i)}\exp(\mathrm{i}k_0\alpha x_2) \times \frac{(w_{11}+w_{12}\gamma_s)\cosh\xi + (w_{21}+w_{22}\gamma_s)\gamma_\nu^{-1}\sinh\xi}{(p_{11}+p_{12}\gamma_s)\zeta + p_{21} + p_{22}\gamma_s},$$
$$\mathcal{E}_2 = 2n_0\zeta E_p^{(i)}\exp(\mathrm{i}k_0\alpha x_2) \times \frac{\left(w_{33}\gamma_s - w_{34}n_s^2\right)\cosh\xi - \left(w_{43}\gamma_s - w_{44}n_s^2\right)n_\nu^{-2}\gamma_\nu\sinh\xi}{\left(p_{33}\gamma_s - p_{34}n_s^2\right)n_0^2 - \left(p_{43}\gamma_s - p_{44}n_s^2\right)\zeta},$$
$$\mathcal{E}_3 = -2n_0\alpha\zeta E_p^{(i)}\exp(\mathrm{i}k_0\alpha x_2) \times \frac{\left(w_{33}\gamma_s - w_{34}n_s^2\right)\gamma_\nu\sinh\xi - \left(w_{43}\gamma_s - w_{44}n_s^2\right)n_\nu^{-2}\cosh\xi}{\left(p_{33}\gamma_s - p_{34}n_s^2\right)n_0^2 - \left(p_{43}\gamma_s - p_{44}n_s^2\right)\zeta}, \tag{5}$$

where $\gamma_\nu = \left(n_\nu^2 - \alpha^2\right)^{1/2}$, n_ν is the refractive index of the layer, $\xi = \mathrm{i}k_0\gamma_\nu x_3$, and x_3 is supposed to be zero at that interface, which is closer to the origin of the coordinate system (Fig. 1). It is not difficult to check that these components obey the conventional boundary conditions. The field $\boldsymbol{\mathcal{E}}$ given by (5) will appear (in Sect. 3) in definitions of volume and surface nonlinear polarisations. Since components of the relevant susceptibility tensors are very small, we intentionally have excluded relatively small contributions to $\boldsymbol{\mathcal{E}}$ that are associated with MO parameters.

Analytical expressions (4) cover a great variety of optically isotropic multilayers and allow us to provide a comprehensive formulation of MOKE. The state of polarisation of the reflected wave, i.e. the Kerr angle θ and the ellipticity η, is defined through the parameter $\chi = E_p^{(r)}/E_s^{(r)}$, provided that the direction of s-polarisation is chosen as a reference in measuring θ. The required relations are [5, 9]:

$$\eta = {}^1\!/_2 \arcsin\left(2\,\mathrm{Im}\chi\left(1+|\chi|^2\right)^{-1}\right),$$
$$\theta = \begin{cases} \theta^* = {}^1\!/_2 \arctan\left(2\,\mathrm{Re}\chi\left(1-|\chi|^2\right)^{-1}\right), & \text{if } |\chi| \le 1, \\ {}^\pi\!/_2\,\mathrm{sgn}\,\mathrm{Re}\chi + \theta^*, & \text{if } |\chi| > 1. \end{cases} \tag{6}$$

When the direction of p-polarisation is chosen, then $\chi = -E_s^{(r)}/E_p^{(r)}$. If the incident wave is either s- or p-polarised, the simple expression $\theta + \mathrm{i}\eta \approx \chi$ for the complex Kerr angle is valid. The positive sign of $\eta \in (0, \pi/4)$ indicates left elliptical polarisation. This means that the electric field rotates around the ellipse in an anticlockwise sense, viewed opposite the wave vector $\boldsymbol{k}^{(r)}$ (Fig. 1). The contrary rotation in the case of $\eta \in (-\pi/4, 0)$ suggests right elliptical polarisation. If $\eta = \pm\pi/4$, the wave is left (right) circularly polarised. The linearly polarised wave corresponds to $\eta = 0$.

The state of polarisation of the reflected and incident waves is the same, if each magnetic layer is set in the transverse configuration ($\boldsymbol{m}_\nu = (1, 0, 0)$, $\nu = 1, ..., J$) and the incident wave is either s- or p-polarised. According to (4), only the p-polarised reflected wave is sensitive to magnetisation, and its intensity changes as the magnetisation is reversed. This is known as transverse MOKE. It can conveniently be characterised by the parameter $\delta = \left(I^+ - I^-\right)/\left(I^+ + I^-\right)$ defined by the intensities for the two opposite magnetisation directions.

To exemplify the theory of MOKE outlined above, the simple configuration with $J = 1$ is worth considering in the linear approximation with respect to thickness (ultrathin-film limit). Equation (4) yields

$$r_{ss}=\frac{\zeta-\gamma_s}{\zeta+\gamma_s}+\frac{2\mathrm{i}k_0\zeta h}{(\zeta+\gamma_s)^2}\left(n^2-n_s^2\right),$$
$$r_{sp}=\frac{2k_0n_0\zeta Qh}{(\zeta+\gamma_s)\left(n_s^2\zeta+n_0^2\gamma_s\right)}\left[m_2\alpha n_s^2+m_3\gamma_s n^2\right],$$
$$r_{ps}=\frac{2k_0n_0\zeta Qh}{(\zeta+\gamma_s)\left(n_s^2\zeta+n_0^2\gamma_s\right)}\left[-m_2\alpha n_s^2+m_3\gamma_s n^2\right],$$
$$r_{pp}=\frac{n_s^2\zeta-n_0^2\gamma_s}{n_s^2\zeta+n_0^2\gamma_s}+\frac{2\mathrm{i}k_0n_0^2\zeta h}{\left(n_s^2\zeta+n_0^2\gamma_s\right)^2}\times\left[\alpha n_s^2\left(1-n_s^2n^{-2}\right)-\gamma_s^2\left(n^2-n_s^2\right)-2\mathrm{i}m_1\alpha\gamma_s n_s^2 Q\right].$$

The symmetry criterion (2) is obviously fulfilled. If the incident wave is s-polarised, the complex Kerr angle is

$$\theta+\mathrm{i}\eta=\frac{r_{ps}}{r_{ss}}=\frac{2k_0n_0\zeta Qh\left(-m_2\alpha n_s^2+m_3\gamma_s n^2\right)}{(\zeta-\gamma_s)\left(n_s^2\zeta+n_0^2\gamma_s\right)}. \tag{7}$$

In the case of p-polarisation it becomes

$$\theta+\mathrm{i}\eta=-\frac{r_{sp}}{r_{pp}}=-\frac{2k_0n_0\zeta Qh\left(m_2\alpha n_s^2+m_3\gamma_s n^2\right)}{(\zeta+\gamma_s)\left(n_s^2\zeta-n_0^2\gamma_s\right)}. \tag{8}$$

When $\boldsymbol{m}=(0,1,0)$ and $\boldsymbol{m}=(0,0,1)$ these simple expressions describe longitudinal and polar MOKE respectively. In the case of transverse MOKE (when $\boldsymbol{m}=(1,0,0)$ and the incident wave has p-polarisation), the component r_{pp} of the reflection matrix (4) leads to

$$\delta=4k_0n_0^2\alpha\zeta h\,\mathrm{Re}\frac{\gamma_s n_s^2 Q}{n_s^4\zeta^2-n_0^4\gamma_s^2}. \tag{9}$$

Simple formulas (7)–(9) for MOKE in an ultrathin layer on a semi-infinite nonmagnetic substrate are just an illustration. In the case when more complex configurations of the multilayer as well as an arbitrary state of polarisation of the incident wave have to be considered, analytical expressions for MOKE can also be deduced from (4), (5). In general, such expressions are inevitably cumbersome, which makes it more preferable to use a simple algorithm, based on (2), (4), and (6), for numerical analysis of MOKE.

3 Second-harmonic wave and SHMOKE

When considering SHMOKE, the s- and p-components of the second-harmonic wave in the transparent medium have first to be found. The procedure of carrying out this most extensive part of the analysis closely follows that for MOKE as outlined in Sect. 2. Now the problem requires us to solve the wave equation for the electric field $\boldsymbol{E}$ in a particular magnetic layer:

$$\nabla\mathrm{div}\boldsymbol{E}-\nabla^2\boldsymbol{E}=k_{0S}^2\left(\hat{\varepsilon}\boldsymbol{E}+\varepsilon_0^{-1}\boldsymbol{P}^{\mathrm{NV}}\right), \tag{10}$$

where $k_{0S}=\omega_S/c$ is the wave number and, in accordance with (1), $\varepsilon_{ij}(\omega_S)=\tilde{n}^2\left(\delta_{ij}-\mathrm{i}\tilde{Q}e_{ijk}m_k\right)$. All the parameters and fields are defined at ω_S. On finding $\boldsymbol{E}$, the magnetic field becomes available from the equation $\boldsymbol{H}=(\mathrm{i}\omega_S\mu_0)^{-1}\mathrm{curl}\boldsymbol{E}$. Another important equation is $\mathrm{div}\hat{\varepsilon}\boldsymbol{E}=-\varepsilon_0^{-1}\mathrm{div}\boldsymbol{P}^{\mathrm{NV}}$. At the ideal interface the fields $\boldsymbol{E}$ and $\boldsymbol{H}$ must also obey the unconventional boundary conditions [7, 10–12]:

$$\begin{aligned}E_1^+-E_1^-&=-\varepsilon_0^{-1}\partial P_3^{\mathrm{NS}}/\partial x_1,\\H_2^+-H_2^-&=\mathrm{i}\omega_s P_1^{\mathrm{NS}},\\E_2^+-E_2^-&=-\varepsilon_0^{-1}\partial P_3^{\mathrm{NS}}/\partial x_2,\\H_1^+-H_1^-&=-\mathrm{i}\omega_s P_2^{\mathrm{NS}},\end{aligned} \tag{11}$$

where the rule to define fields at surfaces is given in Sect. 2. Thus it is necessary to find the response of the layer to the fields radiated by the volume and surface sources. These sources take over the role of the incident wave and are related to the fundamental field $\boldsymbol{\mathcal{E}}$, given by (5).

Since the layer is assumed centrosymmetric (inversion belongs to the point group that describes symmetry of its crystal structure), $\boldsymbol{P}^{\mathrm{NV}}$ vanishes identically in the electric-dipole approximation, i.e. volume-sensitive SHMOKE is forbidden by symmetry, but it survives and can be taken into account as $P_i^{\mathrm{NV}}=\varepsilon_0\chi_{ijkl}^{\mathrm{NV}}(\boldsymbol{m})\mathcal{E}_j\frac{\partial}{\partial x_k}\mathcal{E}_l$ in the electric-quadrupole approximation [1, 2, 13, 14]. In the decomposition of the nonlinear volume susceptibility tensor $\chi_{ijkl}^{\mathrm{NV}}(\boldsymbol{m})=\tilde{\chi}_{ijkl}+\tilde{\chi}_{ijkln}m_n$ we retain only terms linear in magnetisation and assume no intrinsic symmetry for the polar and axial i-tensors. If the layer is isotropic, the Curie group $\infty\infty m$ describes its symmetry. There are three independent nonlinear optical parameters. Only 60 of the 243 components of the axial tensor are nonzero, six of them being independent [15]. Then $\boldsymbol{P}^{\mathrm{NV}}$ can be written in vector form:

$$\begin{aligned}\varepsilon_0^{-1}\boldsymbol{P}^{\mathrm{NV}}=&\ \chi_{2112}(\boldsymbol{\mathcal{E}},\nabla)\boldsymbol{\mathcal{E}}+\chi_{1122}\boldsymbol{\mathcal{E}}\mathrm{div}\boldsymbol{\mathcal{E}}+1/2\chi_{1212}\nabla(\boldsymbol{\mathcal{E}},\boldsymbol{\mathcal{E}})\\&+\chi_{12131}[[\boldsymbol{q},\nabla],\boldsymbol{\mathcal{E}}]+\chi_{31121}(\boldsymbol{\mathcal{E}},\nabla)\boldsymbol{q}\\&+(\chi_{12131}+\chi_{32111})\boldsymbol{q}\mathrm{div}\boldsymbol{\mathcal{E}}\\&+\chi_{11321}\boldsymbol{\mathcal{E}}\mathrm{div}\boldsymbol{q}+\chi_{12311}(\boldsymbol{q},\nabla)\boldsymbol{\mathcal{E}}\\&+1/2\chi_{31211}[\boldsymbol{m},\nabla](\boldsymbol{\mathcal{E}},\boldsymbol{\mathcal{E}}),\end{aligned} \tag{12}$$

where $\boldsymbol{q}=[\boldsymbol{m},\boldsymbol{\mathcal{E}}]$ stands for a vector product. The nonmagnetic part of $\boldsymbol{P}^{\mathrm{NV}}$ is well known [16], although for a different combination of the involved parameters [2, 14, 17, 18], whilst the magnetic part has just recently been derived [7]. The surface polarisation $\boldsymbol{P}^{\mathrm{NS}}$ appearing in the boundary conditions (11) is induced by the fundamental electric field $\boldsymbol{\mathcal{E}}$ at the surface and is related to the latter through a nonlinear surface-susceptibility tensor [1–7, 17, 19]. However, an ambiguity occurs in setting up such a relationship, since the normal component of $\boldsymbol{\mathcal{E}}$ is discontinuous across the surface. This inevitably leads to uncertainty in choosing the most suitable field to drive surface polarisations. It turns out that the driving field may be chosen arbitrarily, and we prefer the convention [7, 17]

$$P_i^{\mathrm{NS}}=\varepsilon_0\chi_{ijk}^{\mathrm{NS}}\left(\boldsymbol{m}^{\mathrm{S}}\right)F_jF_k,\ \ F_1=\mathcal{E}_1,\ \ F_2=\mathcal{E}_2,\ \ F_3=\varepsilon_0^{-1}\mathcal{D}_3, \tag{13}$$

involving the normal component of the displacement (at the fundamental frequency) to keep the driving field continuous across the surface. The tensor in (13) implies that the surface magnetisation, directed along the unit vector $\boldsymbol{m}^S$, may be different from that in the volume.

Taking into account $\boldsymbol{P}^{\mathrm{NV}}$ makes further analysis fairly cumbersome [2]. Moreover, the idea that this polarisation, being actually a plane wave, has just one wave vector, as assumed in [20], does not seem appropriate because there are at least two plane waves (with different wave vectors) driving the polarisation. Normally, the contribution of $\boldsymbol{P}^{\mathrm{NV}}$ to optical effects in centrosymmetric multilayers is much less pronounced than that associated with the surface polarisations and therefore will be neglected henceforth in this paper. The fact that the MO parameter is small ($|\tilde{Q}| \ll 1$) allows us to use a perturbation method for analysing the normal modes in the layer (i.e. the plane waves that are governed by the homogeneous wave equation). Moreover, since nonlinear surface polarisations are treated as perturbations within the model, the quantities $\tilde{Q} P_i^{\mathrm{NS}}$ may be disregarded. Therefore, (10) becomes $\nabla^2 \boldsymbol{E} + (k_{0S}\tilde{n})^2 \boldsymbol{E} = 0$, and it is accompanied by the boundary conditions (11). It follows from (13), (5), and (11) that in the νth layer the normal modes governed by this wave equation are

$$\begin{aligned}
\boldsymbol{E}^{(1,3)} &= E_{01}^{(1,3)} \exp\left(\mathrm{i}\left(\boldsymbol{k}^{(1,3)}, \boldsymbol{x}\right)\right)(1,0,0),\\
\boldsymbol{H}^{(1,3)} &= Z^{-1} E_{01}^{(1,3)} \exp\left(\mathrm{i}\left(\boldsymbol{k}^{(1,3)}, \boldsymbol{x}\right)\right)(0, \pm\tilde{\gamma}, -\alpha),\\
\boldsymbol{E}^{(2,4)} &= E_{02}^{(2,4)} \exp\left(\mathrm{i}\left(\boldsymbol{k}^{(2,4)}, \boldsymbol{x}\right)\right)\left(0, 1, \mp\alpha\tilde{\gamma}^{-1}\right),\\
\boldsymbol{H}^{(2,4)} &= Z^{-1} E_{02}^{(2,4)} \exp\left(\mathrm{i}\left(\boldsymbol{k}^{(2,4)}, \boldsymbol{x}\right)\right)\left(\mp\tilde{n}^2\tilde{\gamma}^{-1}, 0, 0\right),
\end{aligned}$$

where $\boldsymbol{k}^{(1,3)} = \boldsymbol{k}^{(2,4)} = k_{0\mathrm{S}}(0, \alpha, \pm\tilde{\gamma})$, $\tilde{\gamma} = \left(\tilde{n}^2 - \alpha^2\right)^{1/2}$, and $x_3 = 0$ at the interface $S_{\nu-1}$ (Fig. 1). On incorporating these modes into the boundary conditions (11), we arrive at the following expression for the tangential components at the negative sides of the interfaces $S_{\nu-1}$ and S_ν:

$$\begin{bmatrix} E_1^-(0) \\ ZH_2^-(0) \\ E_2^-(0) \\ ZH_1^-(0) \end{bmatrix} = \hat{\tilde{\boldsymbol{M}}}_\nu^{(0)} \begin{bmatrix} E_1^-(h) \\ ZH_2^-(h) \\ E_2^-(h) \\ ZH_1^-(h) \end{bmatrix} + \mathrm{i}k_{0S}\varepsilon_0^{-1} \begin{bmatrix} 0 \\ -P_{1,\nu-1}^{\mathrm{NS}} \\ \alpha P_{3,\nu-1}^{\mathrm{NS}} \\ P_{2,\nu-1}^{\mathrm{NS}} \end{bmatrix},$$

where the nonmagnetic part of the characteristic matrix (2) is defined for the parameters at the frequency ω_S. Generalisation of this relation over the whole multilayer results in the equation

$$\hat{\boldsymbol{F}} \begin{bmatrix} 0 \\ 0 \\ \tilde{E}_s \\ \tilde{E}_p \end{bmatrix} = \hat{\tilde{\boldsymbol{P}}}^{(0)} \begin{bmatrix} 1 & 0 \\ \tilde{\gamma}_s & 0 \\ 0 & 1 \\ 0 & -\tilde{n}_s^2\tilde{\gamma}_s^{-1} \end{bmatrix} \begin{bmatrix} E_{01}^+ \\ E_{02}^+ \end{bmatrix} + \mathrm{i}k_{0S}\varepsilon_0^{-1} \sum_{\nu=0}^{J} \hat{\tilde{\boldsymbol{S}}}_\nu^{(0)} \begin{bmatrix} 0 \\ -P_{1,\nu}^{\mathrm{NS}} \\ \alpha P_{3,\nu}^{\mathrm{NS}} \\ P_{2,\nu}^{\mathrm{NS}} \end{bmatrix}.$$

Since this is similar to (3), the solution can be written down at once:

$$\tilde{E}_s = \tilde{r}_{ss} u_1 - u_3, \quad \tilde{E}_p = \tilde{r}_{pp}^{(0)} u_2 - u_4, \tag{14}$$

where the diagonal components of the reflection matrix (2) are defined at the frequency ω_S, and the u-parameters are components of the vector

$$\boldsymbol{U} = -\mathrm{i}k_{0\mathrm{S}}\varepsilon_0^{-1} \hat{\boldsymbol{F}}^{-1} \sum_{\nu=0}^{J} \hat{\boldsymbol{S}}_\nu^{(0)} \left(0, -P_{1,\nu}^{\mathrm{NS}}, \alpha P_{3,\nu}^{\mathrm{NS}}, P_{2,\nu}^{\mathrm{NS}}\right)^{\mathrm{T}}.$$

At this stage the s- and p-components of the second-harmonic field become available in terms of all the nonlinear surface polarisations. The polarisations themselves are found from (5) and (13).

Our analysis would be deficient without a suitable example. In the case of a single layer ($J = 1$), useful analytical expressions involving two surface polarisations result from (14):

$$\begin{aligned}
\tilde{E}_s &= \frac{\mathrm{i}k_{0\mathrm{S}}\varepsilon_0^{-1}\left(\xi_1 P_{1,0}^{\mathrm{NS}} + P_{1,1}^{\mathrm{NS}}\right)}{\tilde{\gamma}_s \cosh\tilde{\mu} - \tilde{\gamma}\sinh\tilde{\mu} + \zeta\xi_1},\\
\tilde{E}_p &= -\frac{\mathrm{i}k_{0\mathrm{S}}\varepsilon_0^{-1} n_0}{n_0^2\xi_2 + \zeta\xi_3}\left(\xi_2 P_{2,0}^{\mathrm{NS}} + \alpha\xi_3 P_{3,0}^{\mathrm{NS}} + \tilde{\gamma}_s P_{2,1}^{\mathrm{NS}} + \alpha n_s^2 P_{3,1}^{\mathrm{NS}}\right),
\end{aligned}$$

where
$\xi_1 = \cosh\tilde{\mu} - \tilde{\gamma}_s\tilde{\gamma}^{-1}\sinh\tilde{\mu}$, $\xi_2 = \tilde{\gamma}_s\cosh\tilde{\mu} - \tilde{n}_s^2\tilde{n}^{-2}\tilde{\gamma}\sinh\tilde{\mu}$, $\xi_3 = \tilde{n}_s^2\cosh\tilde{\mu} - \tilde{\gamma}_s\tilde{\gamma}^{-1}\tilde{n}^2\sinh\tilde{\mu}$, and $\tilde{\mu} = \mathrm{i}k_{0\mathrm{S}}\tilde{\gamma}h$. As $h \to \infty$, the layer turns into a semi-infinite medium, and the second-harmonic wave is described by

$$\tilde{E}_s = \frac{\mathrm{i}k_{0\mathrm{S}}\varepsilon_0^{-1}}{\zeta + \tilde{\gamma}} P_1^{\mathrm{NS}}, \quad \tilde{E}_p = -\frac{\mathrm{i}k_{0\mathrm{S}}\varepsilon_0^{-1} n_0}{n^2\zeta + n_0^2\tilde{\gamma}}\left(\tilde{\gamma} P_2^{\mathrm{NS}} + \alpha n^2 P_3^{\mathrm{NS}}\right). \tag{15}$$

This basic result is convenient for looking at features of SHMOKE. According to (5), components of the driving field $\boldsymbol{F}$ involved in the convention (13) become

$$\begin{aligned}
F_1 &= \mathcal{E}_1 = \frac{2\zeta}{\zeta + \gamma} E_s^{(i)},\\
F_2 &= \mathcal{E}_2 = \frac{2n_0\zeta\gamma}{n^2\zeta + n_0^2\gamma} E_p^{(i)},\\
F_3 &= n^2\mathcal{E}_3 = -\frac{2n_0\alpha\zeta n^2}{n^2\zeta + n_0^2\gamma} E_p^{(i)}.
\end{aligned}$$

Now we can turn to examples of SHMOKE, which originate from the dependence of the nonlinear surface-susceptibility tensor on magnetisation. To find the Kerr angle and ellipticity of the second-harmonic wave, the parameter $\chi = -\tilde{E}_s/\tilde{E}_p$ will be used in (6) with reference to p-polarisation. If the incident wave is s-polarised,

$$\chi = \frac{\tilde{n}^2\zeta + n_0^2\tilde{\gamma}}{n_0(\zeta + \tilde{\gamma})} \frac{\chi_{111}^{\mathrm{NS}}}{\tilde{\gamma}\chi_{211}^{\mathrm{NS}} + \alpha\tilde{n}^2\chi_{311}^{\mathrm{NS}}}. \tag{16}$$

The Kerr angle and ellipticity can be observed unless χ_{111}^{NS} is zero. Otherwise, the reflected wave is entirely p-polarised.

If the incident wave is p-polarised,

$$\chi = \frac{\tilde{n}^2\zeta + n_0^2\tilde{\gamma}}{n_0(\zeta + \tilde{\gamma})} \frac{Y_1}{\tilde{\gamma} Y_2 + \alpha\tilde{n}^2 Y_3}, \tag{17}$$

where $Y_i = \chi_{i22}^{\mathrm{NS}} + \alpha^2 n^4\gamma^{-2}\chi_{i33}^{\mathrm{NS}} - 2\alpha n^2\gamma^{-1}\chi_{i23}^{\mathrm{NS}}$. The second-harmonic wave has p-polarisation if $Y_1 = 0$.

In the linear approximation with respect to magnetisation, the surface-susceptibility tensor can be decomposed as $\chi^{\mathrm{NS}}_{ijk}(\boldsymbol{m}^{\mathrm{S}}) = \tilde{\chi}_{ijk} + \tilde{\chi}_{ijkl} m^{\mathrm{S}}_l$. The polar and axial i-tensors in this expression possess the apparent intrinsic symmetry: $\tilde{\chi}_{ijk} = \tilde{\chi}_{ikj}$, $\tilde{\chi}_{ijkl} = \tilde{\chi}_{ikjl}$. Hence the number of the independent components is reduced respectively to 18 and 54. The tilde ($\sim$) here marks the tensors defined in the physical coordinate system, which is transformed into the crystallographic system by clockwise rotation about X_3 (in viewing against this axis) through an angle ψ, the axis X_1 being chosen as a reference for the angle. In accordance with the Neumann principle, further simplification occurs through the invariance of χ_{ijk} and χ_{ijkl} (they are now defined in the crystallographic system) under an ordinary point group that describes crystallographic symmetry of the interface [21–24]. The invariance implies a matrix representation of the group, i.e. an isomorphic group of 3×3 matrices corresponding to the coordinate transformations in accordance with the symmetry operations. Consequently for any matrix $\hat{C}$ belonging to the group the equations

$$\chi_{ijk} = C_{il} C_{jm} C_{kn} \chi_{lmn}\,, \; \chi_{ijkl} = \left(\det \hat{C}\right) C_{im} C_{jn} C_{kp} C_{lq} \chi_{mnpq}$$

hold and signify transformations of the tensors into themselves. Such equations constitute the direct inspection method for simplifying tensors. To ensure maximum simplification, it is sufficient to engage consecutively all the generating matrices of the group [22].

As an example, the (001)-interface of fcc layers described by the group $4mm$ is worth considering. On carrying out the direct inspection method that should engage the generating matrices $\begin{bmatrix} -1 & 0 & 0 \\ 0 & 1 & 0 \\ 0 & 0 & 1 \end{bmatrix}$ and $\begin{bmatrix} 0 & 1 & 0 \\ -1 & 0 & 0 \\ 0 & 0 & 1 \end{bmatrix}$, the surviving tensor components are [7]

$$\chi^{\mathrm{NS}}_{111} = m^{\mathrm{S}}_1 \tilde{\chi}_{1111} - m^{\mathrm{S}}_2 \tilde{\chi}_{2221}\,, \; \chi^{\mathrm{NS}}_{122} = -m^{\mathrm{S}}_1 \tilde{\chi}_{1111} - m^{\mathrm{S}}_2 \tilde{\chi}_{2111}\,,$$
$$\chi^{\mathrm{NS}}_{133} = -m^{\mathrm{S}}_2 \chi_{2331}\,, \; \chi^{\mathrm{NS}}_{123} = m^{\mathrm{S}}_3 \chi_{1233}\,, \; \chi^{\mathrm{NS}}_{113} = \chi_{133}\,,$$
$$\chi^{\mathrm{NS}}_{112} = m^{\mathrm{S}}_1 \tilde{\chi}_{1121} - m^{\mathrm{S}}_2 \tilde{\chi}_{1111}\,, \; \chi^{\mathrm{NS}}_{211} = m^{\mathrm{S}}_1 \tilde{\chi}_{2111} - m^{\mathrm{S}}_2 \tilde{\chi}_{1111}\,,$$
$$\chi^{\mathrm{NS}}_{222} = m^{\mathrm{S}}_1 \tilde{\chi}_{2221} + m^{\mathrm{S}}_2 \tilde{\chi}_{1111}\,, \; \chi^{\mathrm{NS}}_{233} = m^{\mathrm{S}}_1 \chi_{2331}\,,$$
$$\chi^{\mathrm{NS}}_{223} = \chi_{113}\,, \; \chi^{\mathrm{NS}}_{213} = -m^{\mathrm{S}}_3 \chi_{1233}\,,$$
$$\chi^{\mathrm{NS}}_{212} = -m^{\mathrm{S}}_1 \tilde{\chi}_{1111} - m^{\mathrm{S}}_2 \tilde{\chi}_{1121}\,, \; \chi^{\mathrm{NS}}_{311} = \chi_{311}\,, \; \chi^{\mathrm{NS}}_{322} = \chi_{311}\,,$$
$$\chi^{\mathrm{NS}}_{333} = \chi_{333}\,, \; \chi^{\mathrm{NS}}_{323} = m^{\mathrm{S}}_1 \chi_{3231}\,, \; \chi^{\mathrm{NS}}_{313} = -m^{\mathrm{S}}_2 \chi_{3231}\,,$$

where $\tilde{\chi}_{1111} = {}^1\!/\!_4 \Delta \sin 4\psi$, $\tilde{\chi}_{1121} = \chi_{1121} - {}^1\!/\!_2 \Delta \sin^2 2\psi$, $\tilde{\chi}_{2111} = \chi_{2111} - {}^1\!/\!_2 \Delta \sin^2 2\psi$, $\tilde{\chi}_{2221} = \chi_{2221} + {}^1\!/\!_2 \Delta \sin^2 2\psi$, $\Delta = \chi_{2111} - \chi_{2221} + 2\chi_{1121}$, and ψ is the angle between [100] and the axis X_1 (Fig. 1). There are nine independent parameters: three optical and six magneto-optical [15]. The interface is optically isotropic [14], since the optical parameters do not depend on ψ, but magneto-optically anisotropic. The state of polarisation and intensity of second-harmonic light would exhibit a four-fold rotational anisotropy. This effect has been observed in Bi-substituted iron-garnet films [25]. If the linear approximation with respect to magnetisation is not used then, particularly for the in-plane magnetisation $\boldsymbol{m}^{\mathrm{S}} || [110]$, invariance of the tensor $\chi^{\mathrm{NS}}_{ijk}\left(\boldsymbol{m}^{\mathrm{S}}\right)$ under the magnetic point group $m\underline{m}\underline{2}$ has to be considered. This invokes 10 independent parameters [19].

For the (001)-interface, (16) yields the following explicit dependence of χ on both MO parameters and ψ:

$$\chi = \frac{\tilde{n}^2 \zeta + n_0^2 \tilde{\gamma}}{\alpha n_0 \tilde{n}^2 (\zeta + \tilde{\gamma}) \chi_{311}} \times \left[{}^1\!/\!_4 m^{\mathrm{S}}_1 \Delta \sin 4\psi - m^{\mathrm{S}}_2 \left(\chi_{2221} + {}^1\!/\!_2 \Delta \sin^2 2\psi\right)\right] . \tag{18}$$

On comparing this with (7), it is not difficult to see that for s-polarisation of the incident wave, SHMOKE is quite different from MOKE. Indeed, for the polar configuration ($\boldsymbol{m}^{\mathrm{S}} = (0, 0, 1)$), (18) predicts the Kerr angle and ellipticity to be both zero, whilst they may be not zero for the transverse configuration ($\boldsymbol{m}^{\mathrm{S}} = (1, 0, 0)$). If the incident wave is p-polarised, in accordance with (17) the χ-parameter may be explicitly expressed as

$$\chi = \frac{\tilde{n}^2 \zeta + n_0^2 \tilde{\gamma}}{\alpha n_0 (\zeta + \tilde{\gamma})} \times \frac{m^{\mathrm{S}}_1 \tilde{\chi}_{1111} + m^{\mathrm{S}}_2 \left(\tilde{\chi}_{2111} + \alpha^2 n^4 \gamma^{-2} \chi_{2331}\right) + 2 m^{\mathrm{S}}_3 \alpha n^2 \gamma^{-1} \chi_{1233}}{2 n^2 \gamma^{-1} \tilde{\gamma} \chi_{113} - \left(\chi_{311} + \alpha^2 n^4 \gamma^{-2} \chi_{333}\right) \tilde{n}^2} . \tag{19}$$

This suggests that variations in the state of polarisation of the second-harmonic wave are possible for all the three conventional configurations. For instance, the Kerr angle and the ellipticity appear for the transverse configuration, unless $\psi = 0$. Equations (18) and (19) also show that SHMOKE (associated with variations in the state of polarisations) exhibits a four-fold rotational anisotropy. Such anisotropy is specific to SHMOKE. It does not exist for structurally isotropic surfaces. Their symmetry is described by the Curie group ∞m which makes the parameter Δ in the above formulas vanish [7]. Many other known nonlinear surface-susceptibility tensors relevant to different symmetry properties of interfaces can be used in the general analysis of SMOKE as outlined above.

4 Conclusion

New analytical solutions to the problem of phenomenological consideration of linear and second-harmonic magneto-optical Kerr effects in ferromagnetically ordered centrosymmetric multilayers have been obtained. The model used implies that the response of the medium is adequately described in terms of surface and volume electric polarisations and that all the interfaces are ideal surfaces (infinitely thin). Since nonlinear polarisations are small, MOKE and SHMOKE can be considered separately. For SHMOKE in centrosymmetric multilayers, the polarisations are related within electric-dipole and -quadrupole approximations to the fundamental field through the surface- and volume-susceptibility tensors, respectively. Examples of such relations have been given in the linear approximation with respect to magnetisation, which allows simplification of the corresponding polar and axial i-tensors to be revealed through their invariance under ordinary point groups describing crystallographic symmetry of the layers and interfaces. An essential and noteworthy feature of the model is that there exist two versions of boundary conditions, which involve a surface polarisation. The conditions we prefer (for they clearly distinguish volume and surface polarisations [7]) are described by (11). An alternative set of boundary conditions [7, 26, 27]:

$$\begin{aligned} &E_1^+ - E_1^- = -\left(\varepsilon_0 \varepsilon_{33}^+\right)^{-1} \partial P_3^{\mathrm{NS}} / \partial x_1, \\ &H_2^+ - H_2^- = \mathrm{i}\omega_{\mathrm{S}} \left(P_1^{\mathrm{NS}} - \varepsilon_{13}^+ / \varepsilon_{33}^+ P_3^{\mathrm{NS}}\right), \\ &E_2^+ - E_2^- = -\left(\varepsilon_0 \varepsilon_{33}^+\right)^{-1} \partial P_3^{\mathrm{NS}} / \partial x_2, \\ &H_1^+ - H_1^- = -\mathrm{i}\omega_{\mathrm{S}} \left(P_2^{\mathrm{NS}} - \varepsilon_{23}^+ / \varepsilon_{33}^+ P_3^{\mathrm{NS}}\right), \end{aligned} \tag{20}$$

which combines the surface polarisation with the dielectric tensor of the layer, may lead to different results.

Another feature of the model is an uncertainty in the definition of the surface polarisation in terms of susceptibility tensor and fundamental electric field, because the normal component of this field is discontinuous across an ideal interface. This problem is resolved by adopting a particular convention. The convention we used is described by (13). Alternatively, for the same surface polarisation two other conventions are possible:

$$\begin{aligned} &P_i^{\mathrm{NS}} = \varepsilon_0 \chi_{ijk}^{\mathrm{NS}+} \left(\boldsymbol{m}^{\mathrm{S}}\right) \mathcal{E}_j^+ \mathcal{E}_k^+, \\ &P_i^{\mathrm{NS}} = \varepsilon_0 \chi_{ijk}^{\mathrm{NS}-} \left(\boldsymbol{m}^{\mathrm{S}}\right) \mathcal{E}_j^- \mathcal{E}_k^- . \end{aligned} \tag{21}$$

Here $\mathcal{E}_i^+$ and $\mathcal{E}_i^-$ are components of the field $\boldsymbol{\mathcal{E}}$ at the positive and negative sides of the interface, respectively, as defined by the positive direction of unit normal $\boldsymbol{N}$. If the off-diagonal components of the dielectric tensor are so small that their contributions to the driving field can be neglected, the tensors χ_{ijk}^{NS}, $\chi_{ijk}^{\mathrm{NS}+}$, and $\chi_{ijk}^{\mathrm{NS}-}$ are simply related to one another:

$$\begin{aligned} &\chi_{ijk}^{\mathrm{NS}} = \chi_{ijk}^{\mathrm{NS}+} = \chi_{ijk}^{\mathrm{NS}-},\ j,k \neq 3, \\ &\chi_{ij3}^{\mathrm{NS}} = \chi_{ij3}^{\mathrm{NS}+} / \varepsilon_{33}^+ = \chi_{ij3}^{\mathrm{NS}-} / \varepsilon_{33}^-,\ j \neq 3, \\ &\chi_{i33}^{\mathrm{NS}} = \chi_{i33}^{\mathrm{NS}+} / \left(\varepsilon_{33}^+\right)^2 = \chi_{i33}^{\mathrm{NS}-} / \left(\varepsilon_{33}^-\right)^2 . \end{aligned} \tag{22}$$

Definitions of the surface polarisation involved in the boundary conditions (20) are obviously similar to those given by (13) and (21). In particular, for the convention $P_i^{\mathrm{NS}} = \varepsilon_0 \eta_{ijk}^{\mathrm{NS}+} \left(\boldsymbol{m}^{\mathrm{S}}\right) \mathcal{E}_j^+ \mathcal{E}_k^+$ the relationship between $\chi_{ijk}^{\mathrm{NS}+}$ and $\eta_{ijk}^{\mathrm{NS}+}$ is rather simple: $\chi_{ijk}^{\mathrm{NS}+} = \eta_{ijk}^{\mathrm{NS}+}$, $i \neq 3$; $\chi_{3jk}^{\mathrm{NS}+} = \eta_{3jk}^{\mathrm{NS}+} / \varepsilon_{33}^+$. The rescaling procedure for the tensors $\eta_{ijk}^{\mathrm{NS}+}$, $\eta_{ijk}^{\mathrm{NS}+}$, and $\eta_{ijk}^{\mathrm{NS}+}$ is exactly the same as that described by (22). Therefore, within the approximation we use, both sets of boundary conditions, (11) and (20), deliver the same results. It is absolutely essential however to state clearly which boundary condition and which convention on the surface polarisation are used.

Finally, the analytical results we have given for the reflected and second-harmonic waves comprise an effective algorithm for numerical analysis of MOKE and SHMOKE in a multilayer. The pursued linear approximation with respect to magnetisation has been shown to be advantageous, particularly in view of the simplicity it presents for looking at rotational anisotropy of SHMOKE. In addition, it also delivers a significantly lower number of nonzero tensor components than would otherwise come from the often-used invariance under magnetic point groups. This has been exemplified for a single interface whose symmetry is described by the group $4mm$, although the susceptibility tensors being invariant under many other point groups can be invoked. The simple expressions we have given for a particular configuration of the multilayer allow a variety of MO effects to be easily analysed. On the whole, a methodologically clear approach, set up in this paper, allows both MOKE and SHMOKE in multilayers to be dealt with unambiguously.

ACKNOWLEDGEMENTS This work was supported by the Royal Society and the EPSRC under Grants Nos. GR/M45566 and GR/N35045. The authors also acknowledge their participation in a recent EPSRC Nonlinear Magneto-optics Network coordinated by Prof. A.D. Boardman.

REFERENCES

1 Y.R. Shen: *The Principles of Nonlinear Optics* (Wiley, New York 1984)
2 N. Bloembergen: *Nonlinear Optics* (Addison-Wesley, Redwood City 1991)
3 W. Hübner: in *Nonlinear Optics in Metals*, ed. by K.H. Bennemann (Clarendon, Oxford 1998) p. 265
4 H.A. Wierenga, M.W.J. Prins, Th. Rasing: Physica B **204**, 281 (1995)
5 N.F. Kubrakov, R. Atkinson: IEEE Trans. Magn. **37**, 2420 (2001)
6 A.V. Petukhov, Th. Rasing: Surf. Sci. **402–404**, 360 (1998); A.V. Petukhov, A. Kirilyuk, Th. Rasing: Phys. Rev. B **59**, 4211 (1999)
7 R. Atkinson, N.F. Kubrakov: Phys. Rev. B **65**, 014432 (2001)
8 A.L. Shelankov, G.E. Pikus: Phys. Rev. B **46**, 3326 (1992)
9 R.M.A. Azzam, N.M. Bashara: *Ellipsometry and Polarized Light* (North-Holland, Amsterdam 1977)
10 M. Idemen: J. Phys. Soc. Jpn. **59**, 71 (1990)
11 A.K. Zvezdin, V.A. Kotov: *Modern Magneto-Optics and Magneto-Optical Materials* (IOP, Bristol 1997); A.K. Zvezdin: Physica A **241**, 444 (1997)
12 B.U. Felderhof, G. Marowsky: Appl. Phys. B **43**, 161 (1987)
13 D.A. Koos, V.L. Shannon, G.L. Richmond: Phys. Rev. B **47**, 4730 (1993); E. Adler: Phys. Rev. **134**, A728 (1964)
14 J.E. Sipe, D.J. Moss, H.M. van Driel: Phys. Rev. B **35**, 1129 (1987)
15 S. Kielich, R. Zawodny: Opt. Acta **20**, 867 (1973)
16 S.A. Akhmanov, V.I. Emel'yanov, N.I. Koroteev, V.N. Seminogov: Usp. Fiz. Nauk **147**, 675 (1985) [Sov. Phys. Usp. **28**, 1084 (1985)]
17 P. Guyot-Sionnest, W. Chen, Y.R. Shen: Phys. Rev. B **33**, 8254 (1986); P. Guyot-Sionnest, Y.R. Shen: Phys. Rev. B **35**, 4420 (1987)
18 H.W.K. Tom, T.F. Heinz, Y.R. Shen: Phys. Rev. Lett. **51**, 1983 (1983)
19 Ru-Pin Pan, H.D. Wei, Y.R. Shen: Phys. Rev. B **39**, 1229 (1989)
20 D.S. Bethune: J. Opt. Soc. Am. B **8**, 367 (1991)
21 N.N. Akhmediev, S.B. Borisov, A.K. Zvezdin, I.L. Lyubchanskii, Y.V. Melikhov: Fiz. Tverd. Tela **27**, 1075 (1985) [Sov. Phys. Solid State **27**, 650 (1985)]
22 R.R. Birss: *Symmetry and Magnetism* (North-Holland, Amsterdam 1964)
23 R.V. Pisarev: Zh. Eksp. Teor. Fiz. **58**, 1421 (1970) [Sov. Phys. JETP **31**, 761 (1970)]
24 M. Lax: *Symmetry Principles in Solid State and Molecular Physics* (Wiley, New York 1974)
25 Th. Rasing: in *Nonlinear Optics in Metals*, ed. by K.H. Bennemann (Clarendon, Oxford 1998) p. 132; V.V. Pavlov, R.V. Pisarev, A. Kirilyuk, Th. Rasing: Phys. Rev. Lett. **78**, 2004 (1997)
26 B. Jérôme, Y.R. Shen: Phys. Rev. E **48**, 4556 (1993)
27 A.K. Zvezdin, N.F. Kubrakov: Zh. Eksp. Teor. Fiz. **116**, 141 (1999) [JETP **89**, 77 (1999)]